Optimisation of the coupling between the ESS accelerator and target: sensitivity to the proton beam profile

Konstantin Batkov, Ferenc Mezei, Alan Takibayev, Luca Zanini
European Spallation Source ESS AB, Tunavägen 24, Lund, Sweden

Abstract. Starting operations in 2019, the European Spallation Source (ESS) will be a pulsed neutron source with an unprecedented brightness, thanks to a 5 MW proton beam (2.5 GeV at 2 mA) impinging on a high-density target. The neutronic optimization is at the core of the work and must take into account the many challenges that a 5 MW proton beam power presents in terms of heat deposition, radiation damage, fatigue, and so on. In this work an optimization study of the coupling of the beam parameters and the target is presented, taking also into account some of the engineering constraints, in particular the heat load on the moderators, on the target, and the peak current density in the proton beam window.

1. Introduction

The European Spallation Source is set to start construction in 2013 and deliver the first neutrons in 2019. ESS will be a long pulse neutron source of 5 MW power, delivering neutrons to 22 independent instruments, for various studies of materials. At present the work is dedicated to a design update, which will results in a Technical Design Report at the end of 2012.

The shape and footprint of the proton beam affect important parameters of the target station, such as its neutronic performance, material damage and cooling. The latter two parameters define the engineering constraints which limit the possible configurations of proton beam profile. The following constraints have been studied in this paper:

- Peak current density in the proton beam window;
- Maximal heat load density in the tungsten wheel;
- Moderator heat load.

These items should be kept as small as possible, without too large penalty in the neutronic performance, so a constrained optimisation has to be performed in order to achieve maximal neutronic performance.

2. Methodology

2.1. Computer codes and data libraries

The Monte Carlo simulations have been performed using the `PHITS` 2.30 [1] and `MCNPX` 2.7 [2] codes coupled with ENDF/B-VII data libraries [3]. In case of `MCNPX`, nuclear interactions outside the libraries energy range were modelled by the Bertini model [4], and in case of `PHITS` — by the JAM model [5].

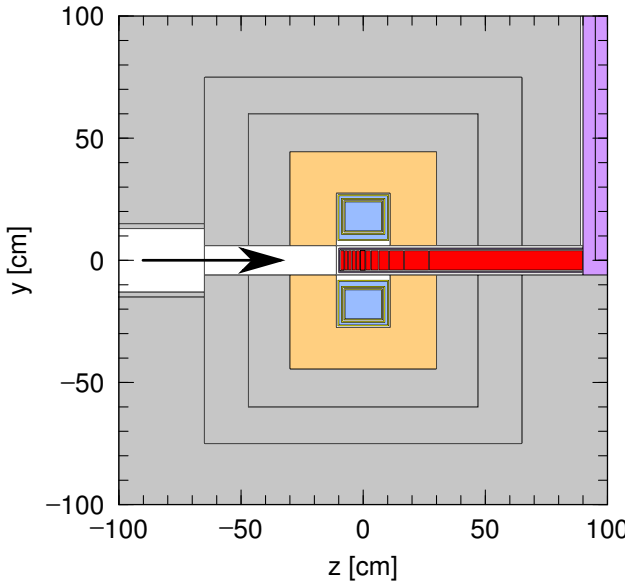

Figure 1: Geometry of TMRA. The arrow shows the proton beam direction. Red: target wheel; Blue: cryogenic moderators; Amber: inner reflector; Gray: outer reflector; Violet: shaft.

2.2. Geometry

In order to analyse the neutronics of the target-moderator-reflector assembly (TMRA), a Monte Carlo model has been developed. This model is based on the ESS Target Station Design Update baseline [6]. It consists of a cylindrical tungsten target and two coupled cryogenic moderators in wing configuration with the main parameters listed in Table 1 and depicted in Fig. 1.

Table 1: Main baseline parameters of TMRA and proton beam.

Target wheel spallation material	Tungsten
Target wheel tungsten height	8 cm
Target wheel coolant	Helium
Target wheel diameter	2.5 m
Moderator shape	Cylindrical
Moderator radius (inner vessel dimension)	8 cm
Moderator height (inner vessel dimension)	13 cm
Moderator fluid	Para-H_2
Moderator temperature	20 K
Inner reflector material	Beryllium
Inner reflector radius	60 cm
Outer reflector material	Steel
Proton beam kinetic energy	2.5 GeV
Proton beam profile	2D parabolic
Proton beam full height	6 cm
Proton beam full width	16 cm

Table 2: Input parameters for the Monte Carlo mesh simulations

	Unit	Min	Max	Step
Proton Beam Width	cm	0	8	0.5
Proton Beam Height	cm	0	25	0.5

2.3. Sensitivity analysis

In order to study how neutronic performance and engineering parameters depend on the beam profile, a separate Monte Carlo run has been performed for every proton beam profile configuration. These configurations are summarised in Table 2: both proton beam width and height were changed between the corresponding minimal and maximal values with the step of 0.5 cm. The following output values were recorded in each run:

- Neutronic performance (defined in Sec. 2.5);
- Peak current density in the proton beam window;
- Maximal heat load density in the tungsten wheel;
- Moderator heat load.

2.4. Proton beam profile

Two proton beam profile options have been studied: two dimensional (2D) parabolic and uniform. Both distributions can be defined by the full widths in x- and y-directions, A and B, respectively.

2D Parabolic The probability density function of 2D parabolic profile has been defined as

$$p(x,y) = \frac{9}{16\,AB}\left(1-\frac{x^2}{A^2}\right)\left(1-\frac{y^2}{B^2}\right). \tag{1}$$

Uniform The probability density function of flat profile has been defined as

$$p(x,y) = \begin{cases} (AB)^{-1} & \text{if } |x| \le A \text{ and } |y| \le B; \\ 0 & \text{otherwise.} \end{cases} \tag{2}$$

2.5. Neutronic performance

Neutronic performance has been measured in the units of the cold neutron flux integrated over time, integrated for energies below 5 meV, and extracted from a viewed surface in the centre of the beam extraction channel:

$$\mathrm{FoM} = \int_0^\infty dt \int_0^{5\,\mathrm{meV}} \Phi(t,E)dE. \tag{3}$$

During the optimisation, this value, the brightness of the moderator viewing surface, was considered as the figure of merit (FoM).

In the `MCNPX` simulations the value of FoM was calculated by means of a standard sampling biasing technique of scoring neutron flux at a point detector behind an ideal collimator, followed

Table 3: Optimisation results

(a) Absolute units

	Unit	Baseline	Optimal Parabolic	Optimal Uniform
Proton Beam Height	cm	6	0.01	1
Proton Beam Width	cm	16	3.5	1.5
Moderator Heat Load	kW	10.5 ± 0.2	10.8 ± 0.2	10.7 ± 0.2
Max Heat Load Density in the Wheel	kW/cm^3	3.2 ± 0.2	23.9 ± 0.5	27.7 ± 0.5
Peak Neutron Brightness	n/cm^2/s/sr	$2.03 \cdot 10^{14}$	$2.11 \cdot 10^{14}$	$2.11 \cdot 10^{14}$

(b) Relative units

	Unit	Baseline	Optimal Parabolic	Optimal Uniform
Moderator Heat Load	%	97	100	99
Max Heat Load Density in the Wheel	%	13	100	116
Peak Neutron Brightness	%	96	100	100

by a solid angle correction. In the `PHITS` simulations this value was calculated by means of a surface crossing tally.

Beam divergence between the proton beam window and the target wheel has not been taken into account in this study.

3. Results

The results of optimisation are summarised in Table 3.
It shows the values corresponding to the baseline [6] configuration, as well as the neutronic optimal points in the cases of parabolic and uniform proton beam profiles.

Normalisation In order to make comparison between different beam configurations more visual, last three lines of Table 3a were renormalised in the units of the optimal point found with the parabolic configuration. These renormalised values are summarised in Table 3b.

Optimal point The optimal point with both parabolic and uniform beam profiles was found with an almost pencil-like beam (see Table 3a), which is obviously not feasible due to huge peak current density in the proton beam window. However, the current baseline configuration gives just 4% less performance with respect to the pencil beam, but lowers down the peak current density to a reasonable value of 47 μA/cm^2.

Note that the engineering parameters do not change significantly between the baseline configuration and the optimal parabolic and uniform cases.

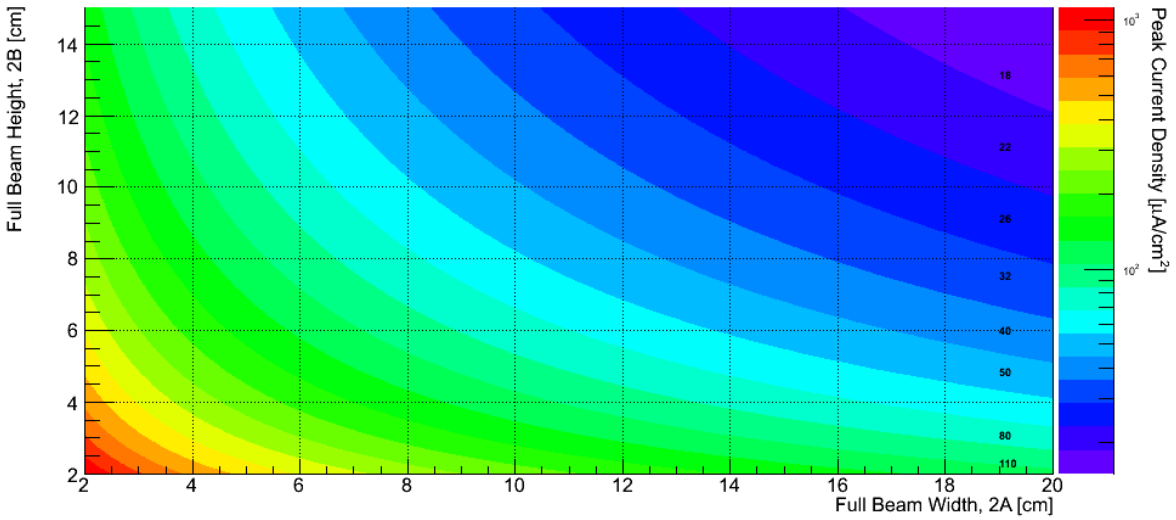

Figure 2: Peak current density as a function of 2D parabola dimensions

3.1. Peak current density in the proton beam window

The peak current densities can be derived from the corresponding probability density functions:

$$\text{Uniform:} \quad \mathcal{I}_u = \frac{C}{A \cdot B}, \tag{4}$$

$$\text{Parabolic:} \quad \mathcal{I}_p = \frac{C}{A \cdot B} \cdot \frac{9}{16} \propto \mathcal{I}_u, \tag{5}$$

where $C = 2\,\text{mA}$ is time averaged proton beam current.

Fig. 2 shows the peak current density as a function of beam dimensions in the case of parabolic profile. Numbers in different colour bands on the right side of the figure indicate the approximate values of peak current density in $\mu\text{A/cm}^2$ for the particular colour region. These numbers correspond to the colour scale palette plotted nearby. Due to Eq. (5), the peak current densities of 2D parabolic and uniform profiles are proportional to each other, so the corresponding figure for the uniform profile can be obtained by a linear scaling of Fig. 2.

3.2. Neutronic performance

Neutronic performance as a function of proton beam dimensions is shown in Fig. 3 for both proton beam shape options. A black marker ● in Fig. 3a corresponds to the baseline settings (see Table 3). As in the case of peak current density, one can observe a linear dependency between both beam profile shapes (compare figures 3a and 3b).

Fig. 4a is a one-dimensional analogue of Fig. 3a, where the x-axis values were calculated with eq. (5). The spread along the y-axis in Fig. 4a is caused by the fact that the same peak current density can be obtained with different combinations of beam dimensions. The baseline configuration is shown by ● . The black dots in Fig. 4b were calculated from Fig. 4a by averaging the spread along the y-axis. Despite the fact that this is a biased average calculation, it gives a visual estimate how neutronic performance depends on the peak current density. Note that it asymptotically approaches 100 % performance at the infinite peak current density (pencil-like beam).

The same plot for the uniform beam profile is shown with red points.

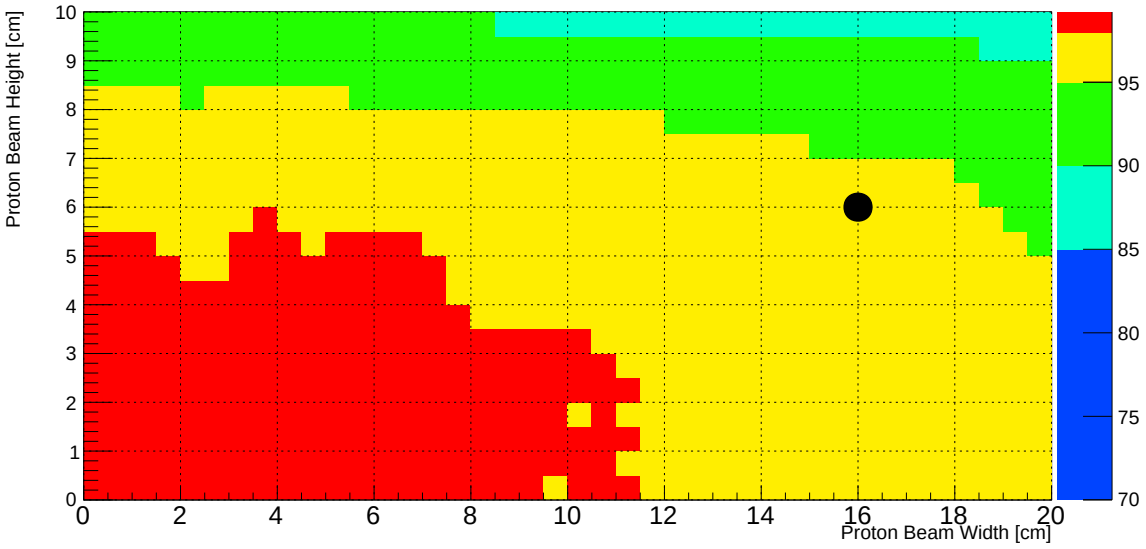

(a) Parabolic profile

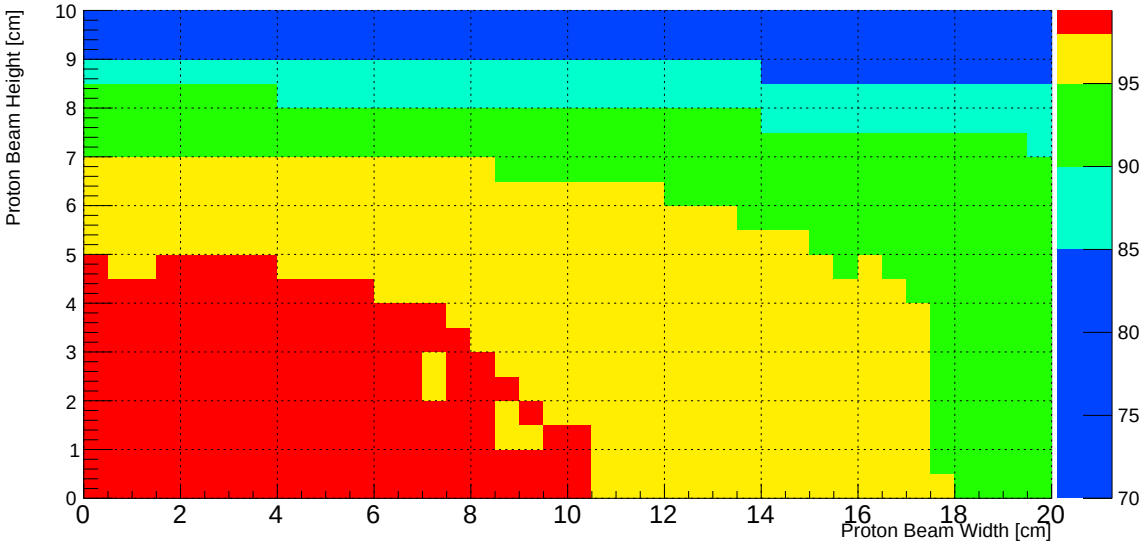

(b) Uniform profile

Figure 3: Neutronic performance as a function of proton beam dimensions

Fig. 4b concludes that for a given peak current density there is no pronounced difference between the parabolic and uniform beam profiles from the point of view of neutronic performance.

The figures in the following sections have been obtained by the same procedures, so they will not be described in detail.

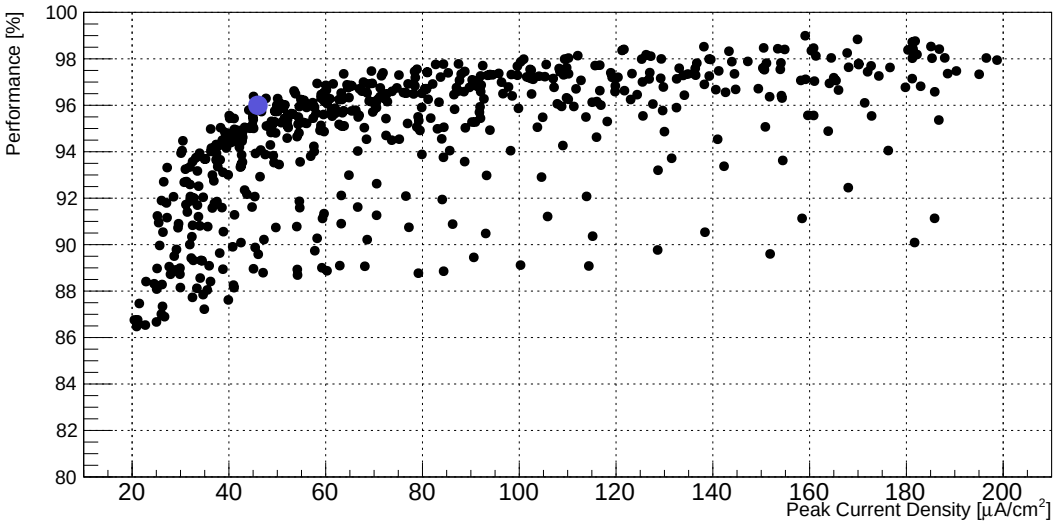

(a) Neutronic performance as a function of peak current density in the case of parabolic profile

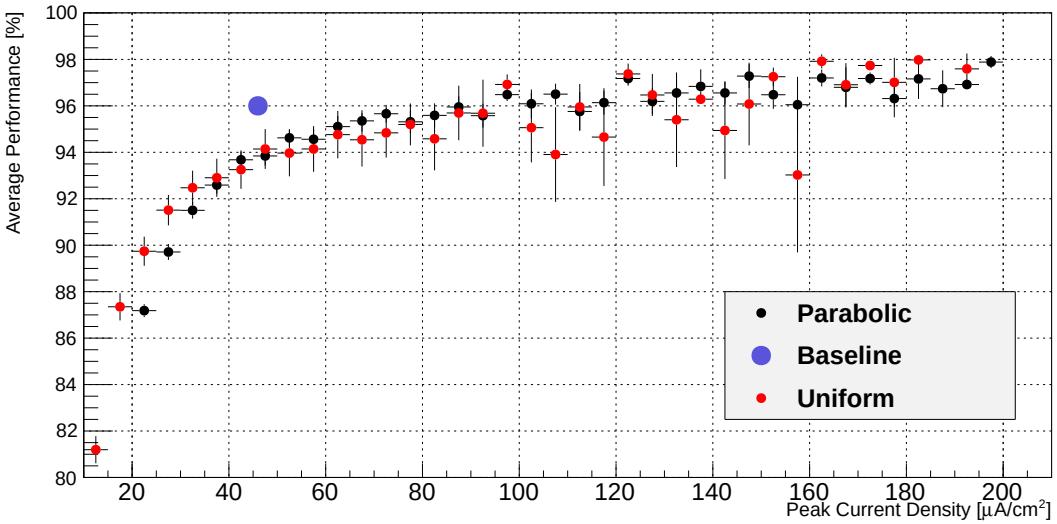

(b) Average neutronic performance as a function of peak current density

Figure 4: Neutronic performance as a function of peak current density

3.3. Moderator heat load

Figures 5 and 6 show the moderator heat load as a function of proton beam dimensions (Fig. 5) and peak current density (Fig. 6). As in the case of neutronic performance, for a given peak current density there is no difference between the parabolic and uniform beam profiles.

3.4. Maximal heat load density in the target wheel

Figures 7 and 8 show the maximal heat load density in the target wheel as a function of proton beam dimensions (Fig. 7) and peak current density (Fig. 8). There is no significant difference between the parabolic and uniform beam profiles.

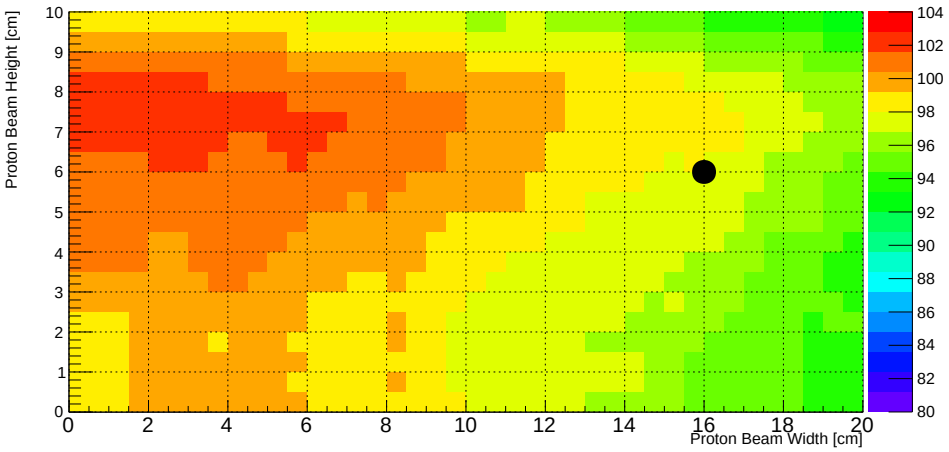

(a) Parabolic profile

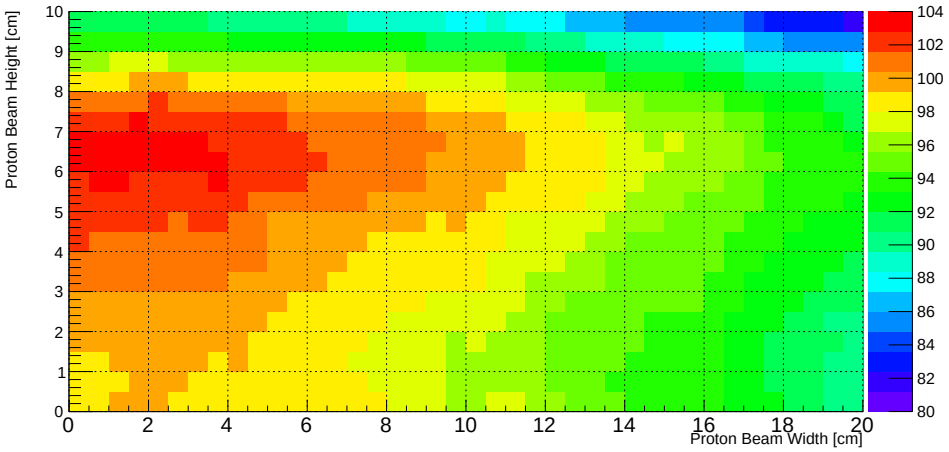

(b) Uniform profile

Figure 5: Moderator heat load as a function of proton beam dimensions

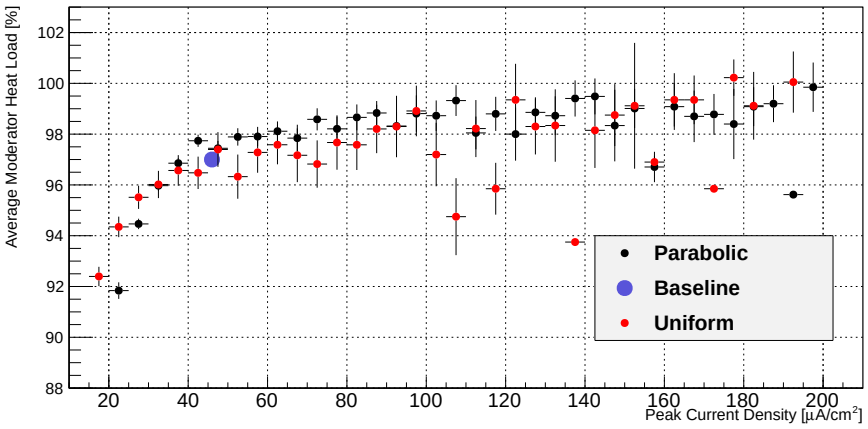

Figure 6: Average moderator heat load as a function of peak current density

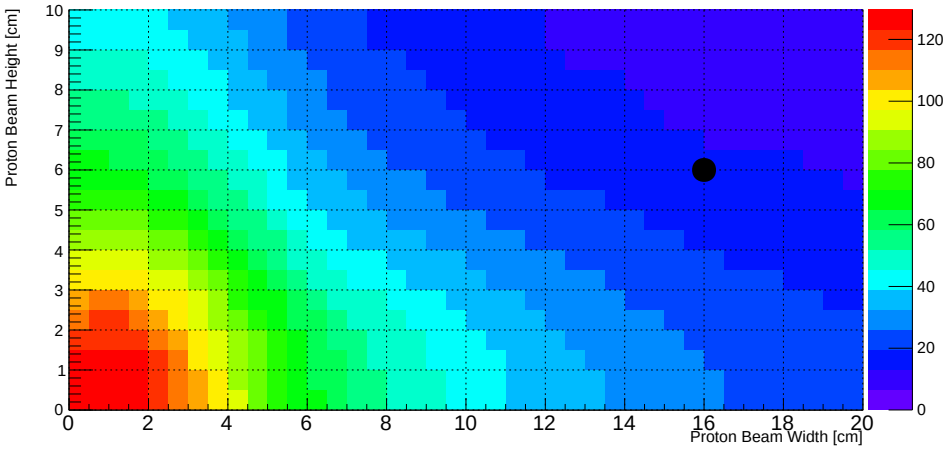

(a) Parabolic profile

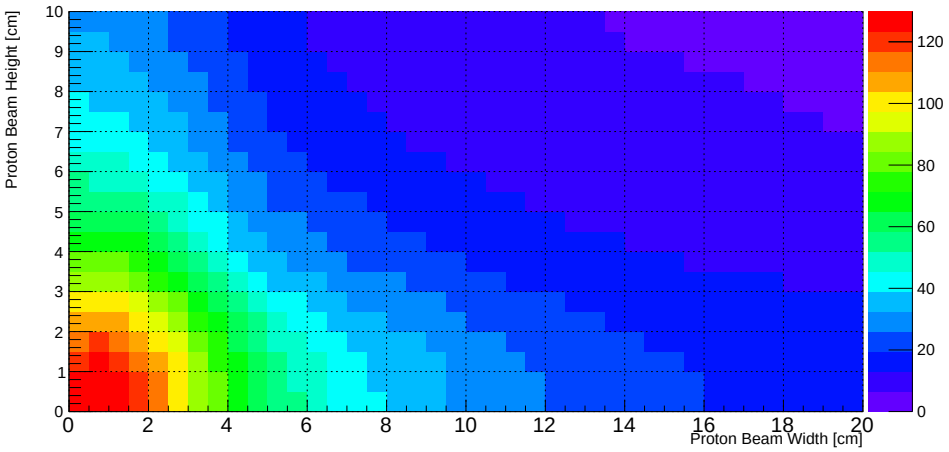

(b) Uniform profile

Figure 7: Maximal heat load density as a function of proton beam dimensions

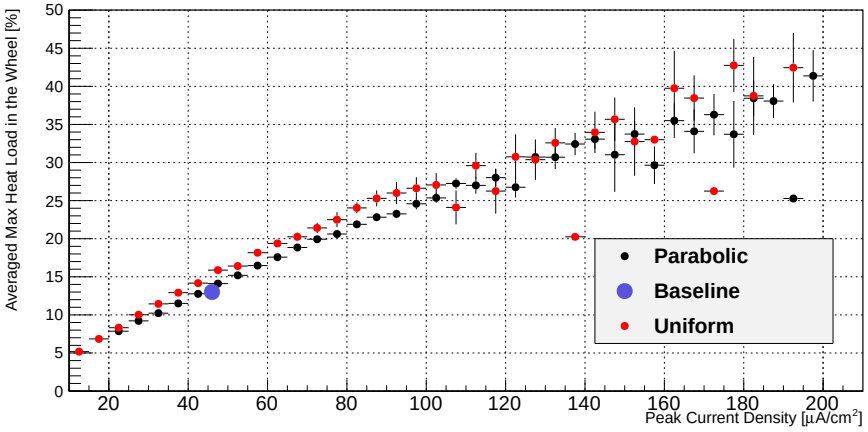

Figure 8: Average maximal heat load density as a function of peak current density

4. Summary

The main results of this optimisation study can be summarized as follows:

- The baseline beam parameters with peak current density of 46 μA/cm^2 give almost the same neutronic performance (96 %) as the optimal value obtained with the pencil-like beam.
- There is no significant difference between parabolic and flat beam profiles from the point of view of neutronic performance and engineering parameters studied in this paper.
- There is a freedom in choosing the proton beam footprint without decreasing neutronic performance and rising engineering constrains.

References

[1] Niita K, Matsuda N, Iwamoto Y, Iwase H, Sato T, Nakashima H, Sakamoto Y and Sihver L. *PHITS: Particle and Heavy Ion Transport code System, Version 2.23*, JAEA-Data/Code 2010-022 (2010).

[2] *MCNPX User's Manual, Version 2.7.0*, ed Pelowitz D B, LA-CP-11-0438 (2011).

[3] Chadwick M B, Oblozinský P, Herman M, Greene N M, McKnight R D, Smith D L, Young P G, MacFarlane R E, Hale G M, Frankle S C, *et al. ENDF/B-VII.0: Next generation evaluated nuclear data library for nuclear science and technology*, *Nuclear data sheets*, 102, 2931–3060 (2006).

[4] Bertini H W *Intrenuclear-cascade calculation of the secondary nucleon spectra from nucleon-nucleus interactions in the energy range 340 to 2900 MeV and comparisons with experiment. Phys. Rev.*, 188(4):1711–1730 (1969).

[5] Nara Y, Otuka N, Ohnishi A, Niita K and Chiba S. *Relativistic nuclear collisions at 10 AGeV energies from p+Be to Au+Au with the hadronic cascade model. Phys. Rev.* C61, 024901 (1999).

[6] *ESS target station design update baseline*, ESS-EDMS1166507 version 2 (2011).